29 May 2010, 8:00 am - 9:30 am

Using Tactile Pressure Sensors to Measure Lateral Spreading Induced Earth Pressures Against a Large, Rigid Foundation

Scott M. Olson
University of Illinois at Urbana-Champaign, IL

Mark R. Muszynski
University of Illinois at Urbana-Champaign, IL

Carmine Polito
Valparaiso University, Valparaiso, IN

Youssef M. A. Hashash
University of Illinois at Urbana-Champaign, IL

Camilo Phillips
University of Illinois at Urbana-Champaign, IL

Fifth International Conference on
Recent Advances in Geotechnical Earthquake Engineering and Soil Dynamics
and Symposium in Honor of Professor I.M. Idriss
May 24-29, 2010 • San Diego, California

USING TACTILE PRESSURE SENSORS TO MEASURE LATERAL SPREADING-INDUCED EARTH PRESSURES AGAINST A LARGE, RIGID FOUNDATION

Scott M. Olson
University of Illinois at Urbana-Champaign, IL 61801, USA

Mark R. Muszynski
University of Illinois at Urbana-Champaign, IL 61801, USA

Carmine Polito
Valparaiso University, Valparaiso Indiana 46383, USA

Youssef M.A. Hashash
University of Illinois at Urbana-Champaign, IL 61801, USA

Camilo Phillips
University of Illinois at Urbana-Champaign, IL 61801, USA

ABSTRACT

Two centrifuge tests were performed at the NEES facility at Rensselaer Polytechnic Institute (RPI) to observe lateral earth pressures mobilized against a rigid foundation element during liquefaction-induced lateral spreading, as part of a larger NEESR study aimed at developing novel approaches to mitigate the effects of seismically-induced ground failures on large, rigid foundation elements. Models were constructed in a laminar box to allow unimpeded downslope soil displacement, and the sand in the model was liquefied during the centrifuge test. Lateral pressures prior to, during, and after shaking and liquefaction were directly measured using a novel device: tactile pressure sensors. Prior to testing the production models, several 1g and centrifuge experiments were conducted to determine whether the tactile pressure sensors would accurately measure pressures. Using the tactile pressure sensor and configuration described in this paper, geostatic pressures measured prior to the shaking agreed well with the anticipated theoretical at-rest earth pressures. In this paper, we describe these initial tests, the challenges that were encountered, methods employed to overcome these challenges, and the production centrifuge tests.

INTRODUCTION

Shaking-induced ground failures (including liquefaction induced lateral spreads) are a major source of damage and economic loss from earthquakes. The design of infrastructure located at sites susceptible to earthquake-induced ground failure often requires designers to determine seismically-induced earth pressures. A few approaches are available to evaluate liquefaction-induced earth pressures against flexible foundations (e.g., single piles or small pile groups); however, many new bridges and other structures employ large, rigid foundations to carry static and seismic loads. For example, the Bill Emerson bridge over the Mississippi River in Cape Girardeau, MO, uses 33.5m x 21m dredged cellular gravity caissons, the New Carquinez Strait Bridge in San Francisco, CA, uses 3m diameter drilled shaft groups, and the Port Mann bridge over the Fraser River in Vancouver, Canada, will use 90 2m diameter concrete-filled pipe pile groups, respectively, to support their main spans. In these cases, little guidance is available for evaluating liquefaction-induced earth pressures against these large, rigid foundations.

As part of an ongoing Network for Earthquake Engineering Simulation (NEES) research project, the project team is in the process of performing a series of centrifuge tests designed to measure liquefaction-induced lateral spreading forces against a large, rigid foundation element and to develop novel ground improvement methods to mitigate the consequences of liquefaction-induced ground failure for these foundations. The latter objective is consistent with the profession's movement toward Performance-Based Design (PBD) and Performance-Based Earthquake Engineering (PBEE).

The centrifuge tests for this project were performed at the NEES 150 g-ton centrifuge facility at Rensselaer Polytechnic Institute (RPI) using an inclined laminar box and fine Nevada sand. In the two production centrifuge tests performed to date, tactile pressure sensors were installed on the upslope face of a rigid foundation element to measure earth pressures imposed by seismic shaking and liquefaction-induced lateral spreading. To our knowledge, these tactile pressure sensors have never been used to measure dynamic earth pressures in a saturated soil. In this new application of these instruments, the project team encountered a number of obstacles in using the sensors in this environment.

In this paper, we describe the challenges associated with implementing the tactile pressure sensors in this environment, the approaches used to overcome these challenges, and the lessons learned from the experiments. In addition, we summarize the tactile pressure sensor results obtained in the most recent test.

CENTRIFUGE TESTING PROGRAM

The initial phase of testing consisted of two centrifuge experiments (Experiments I-A and I-A2 conducted in summer 2008 and 2009, respectively) intended to measure lateral earth pressures against a rigid foundation element during liquefaction-induced lateral spreading. The primary differences between the two tests were the input motion amplitude and duration, instrument placement techniques, and most importantly, major changes to the tactile pressure sensor configurations, as described subsequently. Unless otherwise noted, all dimensions given are in prototype scale.

Input Seismic Demand

The input motion for Experiment I-A consisted of 3 cycles of low amplitude shaking at about 0.01g followed by 30 cycles of strong shaking at about 0.3g. Because this shaking intensity resulted in lateral spreading displacements that reached the limit of the laminar box, we reduced the shaking intensity in Experiment I-A2 to 3 cycles of low amplitude shaking at about 0.01g followed by 20 cycles of strong shaking at about 0.18g. In both experiments, the initial low amplitude cycles are used to calibrate the small-strain behavior of numerical models. Fig. 1 presents the input motions for both tests.

Laminar Box

The tests were performed in a flexible laminar box to allow unrestrained movement in the longitudinal box direction (and in the direction of shaking). The RPI laminar box has internal dimensions of 71 cm × 35.5 cm (in plan) × 26 cm high (maximum). Both models were tested at 50 g.

Rigid Foundation Element

The rigid foundation element (caisson) used in these experiments mimics the behavior of dredged cellular gravity caissons, large pile or drilled shaft groups, or similar large, rigid foundations. The test caisson consists of a thick-walled aluminum box with exterior dimensions of 5 m long × 3.7 m wide × 15.2 m high and is attached to the base of the laminar box using four screws to ensure a fixed connection.

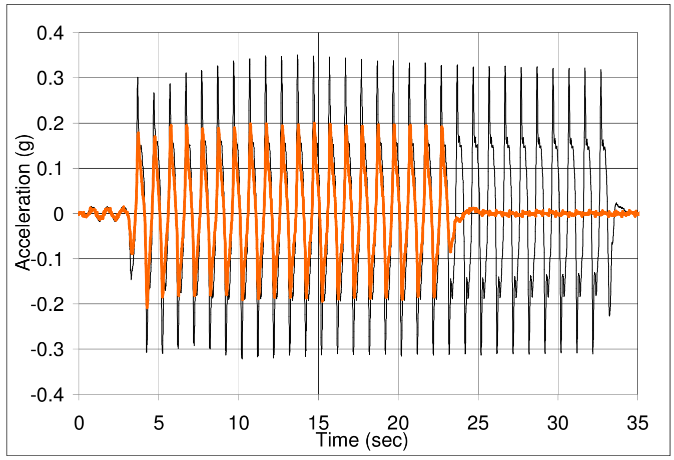

Fig. 1 Input motions for Experiments I-A and I-A2.

Test Sand and Prototype Soil Profile

Nevada sand (No. 120) was used for both tests. Nevada sand is a fine-grained, clean, quartz sand with subrounded to rounded particles. Its median grain size, D_{50}, is 0.15 mm, and reported minimum and maximum void ratios are 0.516 and 0.894, respectively (Arumoli 1992). Loose sand was placed in the laminar box by dry pluviation with a funnel. The sand relative density, D_r, prior to spin-up was between 40 and 45%.

The soil profile consisted of 10 m of loose sand overlying 2 m of dense, lightly cemented sand (leaving over 3 m of the caisson exposed), as illustrated in Figs. 2 and 3. The dense, lightly cemented sand was used to cover the base of the laminar box and aluminum caisson in order to provide a realistic boundary condition at the interface.

The Nevada sand was saturated using demineralized, deaired water. In centrifuge testing, soil permeability scales directly with centrifugal acceleration (Kutter 1995). At 50g, the Nevada sand permeability at D_r ~ 40 to 45% is approximately $2x10^{-3}$ cm/s (Arumoli 1992). This permeability corresponds approximately to a poorly-graded coarse sand at 1g.

Instrumentation

Instrumentation in the models included pressure transducers and accelerometers to measure porewater pressure (PWP) and acceleration at numerous locations throughout the model, linear voltage differential transformers (LVDT) and lasers installed on the rings outside the laminar box to measure lateral displacement with depth, subsurface sand grids and surface tracking markers to measure lateral displacement at discrete locations and depths, as well as tactile pressure sensors to measure lateral earth pressure against the caisson.

The main objective of this paper is to discuss the use of the tactile pressure sensors in the context of geotechnical centrifuge application. Therefore, we will not go into detail regarding the other instrumentation. The instruments, including accelerometers, PWP transducers, LVDTs, and subsurface sand grids, indicated that liquefaction and cyclic mobility occurred in the upper approximate 6 m, and the entire potentially liquefiable stratum experienced substantial increases in pore water pressure during shaking. Values of r_u approached 80% even for the lower portions of the loose stratum.

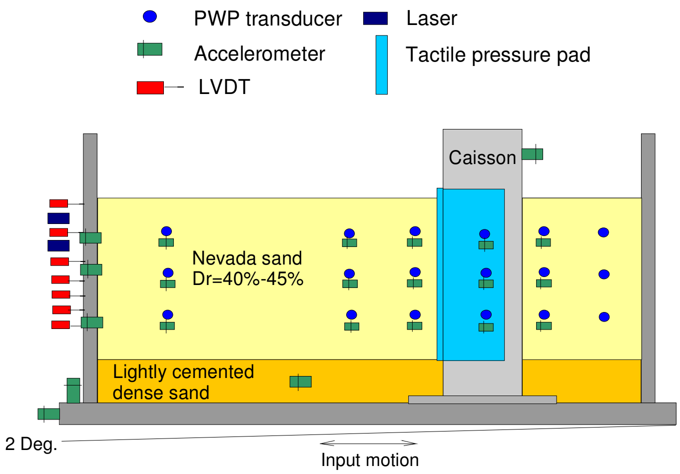

Fig. 2 Soil profile and general instrument configuration for Experiments I-A and I-A2 (sectional view).

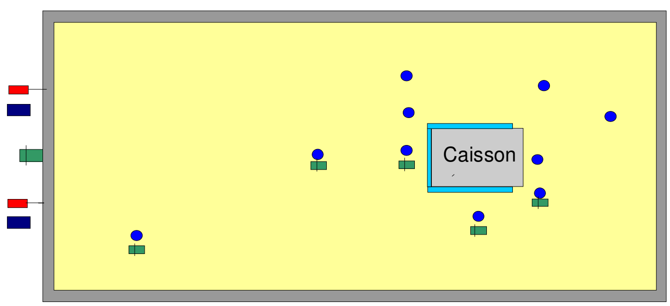

Note: instrumentation is the same for all three layers

Fig. 3 Instrument configuration for Experiments I-A and I-A2 (plan view).

Use of Tactile Pressure Sensors in Centrifuge Testing

Using tactile pressure sensors to measure lateral earth pressures in a saturated, dynamic centrifuge environment has not been attempted previously and, as a result, the project team encountered several challenges. The following sections describe some of these challenges and the solutions developed by the Illinois project team and RPI personnel.

Experiment I-A Tactile Pressure Sensor Configuration. In Experiment I-A, we used two Tekscan, Inc. Model #5101 tactile pressure sensors (see Fig. 4) to measure pressure against the rigid caisson. Because of their relatively small size, two of the Model #5101 sensors were required to cover the upslope face of the caisson in Experiment I-A. The sensors were positioned in series vertically with a slight overlap. Additionally, each sensor was folded over twice to reduce its width so that it would fit on the front face of the caisson. This configuration allowed us to use a rubber membrane to fully encase the sensors and to create a watertight barrier, as illustrated in Fig. 5. The membrane was required because the tactile pressure sensors are negatively affected by water.

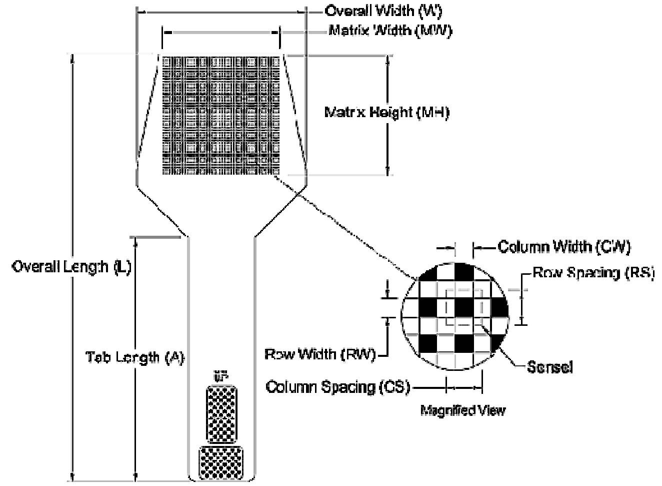

Model	General Dimensions: Overall Length L	Overall Width Width	Tab Length A	Sensing Region Dimensions: Matrix Width MW	Matrix Height MH	CW	CS	Qty.	RW	RS	Qty.	Summary: Total No. of Sensels	Sensel Spatial Resolution
US 5101	(in) 13.39	(in) 5.86	(in) 6.59	(in) 4.40	(in) 4.40	(in) 0.050	(in) 0.100	44	(in) 0.050	(in) 0.100	44	1936	(sensel per sq-in) 100
Metric 5101	(mm) 340.0	(mm) 149.0	(mm) 167.3	(mm) 111.8	(mm) 111.8	(mm) 1.3	(mm) 2.5	44	(mm) 1.3	(mm) 2.5	44	1936	(sensel per sq-cm) 15.5

Fig. 4 Model #5101 tactile pressure sensor used in Experiment I-A.

Despite the efforts to address potential issues with the tactile pressure sensors prior to the test, Experiment I-A yielded pressure measurements that were difficult to interpret, so questions arose regarding the use of an overlap between sensors, folding the sensors, and placing the sensors behind the membrane without adhesive (thereby potentially allowing the sensors to move with respect to the caisson, the sand stratum, and each other.

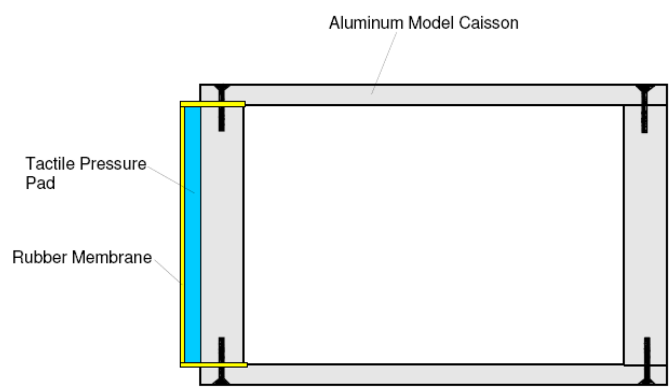

Fig. 5 Plan view of rubber membrane used as a waterproof barrier and tactile pressure sensor configuration employed in Experiment I-A.

Waterproofing the Sensors. After Experiment I-A, RPI began experimenting with alternatives for waterproofing the tactile pressure sensors. The preferred alternative developed by RPI involves laminating each tactile pressure sensor between two clear plastic adhesive sheets. The lamination replaces the rubber membrane used in Experiment I-A. However, the lamination process is not without potential difficulty. The tactile pressure sensors consist of two sheets of Mylar with pressure-sensitive resistive material between. When applying the lamination sheets to the pressure sensors, RPI previously determined that there was a possibility of trapping small amounts of air between the laminating sheets and the outside Mylar material of the pressure sensor. However, by placing the adhesive sheets beginning at one end of the sensor, and moving to the opposite end while applying pressure incrementally to the lamination material on a flat table, this problem was avoided. To prevent air build up inside the sensors (between the Mylar sheets) during application of the adhesive sheets, the tactile pressure sensors are pierced near the top of the handle to allow air to vent while avoiding the resistive strips that must carry a continuous flow of current to operate. The pierced portion (air vent) of the tactile pressure sensor then must be positioned to remain above the water level throughout the testing.

Several tests were conducted at RPI using this lamination procedure, and these tests have shown that similar pressures are measured using both laminated and non-laminated tactile pressure sensors in both dry and saturated conditions. In all of the verification tests, the laminated sensors have saved time, remained watertight, and remained operational. In addition, the laminated sensors can be calibrated using the same technique as the non-laminated sensors.

Updated Tactile Pressure Sensor Model. To avoid potential sensor movement and required folding of the two tactile pressure sensors used in Experiment I-A, as well as to simplify installation, the project team opted to use a larger tactile pressure sensor for the next test (Tekscan, Inc. Model #5250; see Fig. 6) that could cover the entire upslope face of the caisson (as well as cover most of the sides). Use of the larger sensor was only possible with the newly developed sensor lamination process to protect the instrument from water without the need for a rubber membrane.

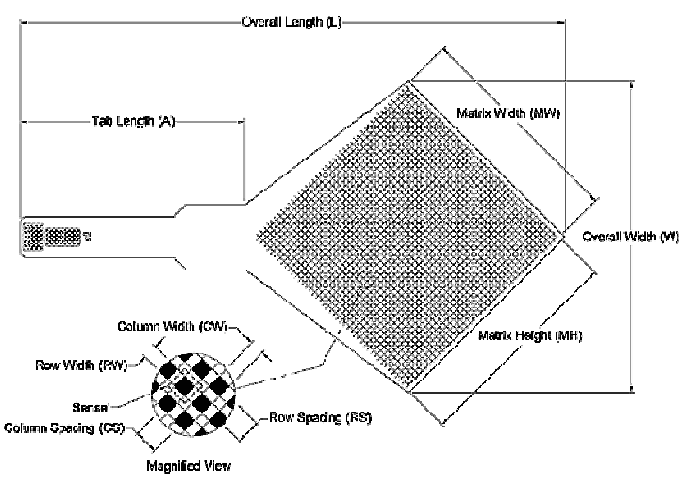

	General Dimensions			Sensing Region Dimensions								Summary	
Model	Overall Length L	Overall Width W	Tab Length A	Matrix Width MW	Matrix Height MH	Columns CW	Columns CS	Columns Qty.	Rows RW	Rows RS	Rows Qty.	Total No.of Sensels	Sensel Spatial Resolution
US	(in)	(in)	(in)	(in)	(in)	(in)	(in)		(in)	(in)			(sensel per sq-in)
5250	24.51	14.11	10.00	9.68	9.68	0.130	0.220	44	0.130	0.220	44	1936	20.7
Metric	(mm)	(mm)	(mm)	(mm)	(mm)	(mm)	(mm)		(mm)	(mm)			(sensel per sq-cm)
5250	622.6	358.3	254.0	245.9	245.9	3.3	5.6	44	3.3	5.6	44	1936	3.2

Fig. 6 Model #5250 tactile pressure sensor.

The Model 5250 sensor has matrix dimensions (i.e., pressure sensing area) of about 600 cm^2 (model scale), approximately five times larger than the Model 5101 (125 cm^2); however, the sensel density is significantly smaller (3.2 sensel/cm^2 for Model 5250 compared to 15.5 sensels/cm^2 for Model 5101). The Model 5250 is rated for a maximum pressure of about 170 kPa (same as Model 5101). The use of this relatively low maximum pressure ensures sensing resolution near the surface, where liquefaction is prevalent.

Measured Geostatic Pressures using the Sensors. Another challenge observed during Experiment I-A was that the sensors measured lateral earth pressures that were consistently and substantially smaller than that predicted by at-rest earth pressure theory. This was observed again in subsequent tests performed by RPI with both laminated and non-laminated sensors. Because the tactile pressure sensors were no longer folded over, and because we believed the calibration technique to be valid, we concentrated on the possibility of shear forces causing a pressure reduction.

The notion of shear forces affecting the tactile pressure sensor measurements has been the subjected of recent research at RPI (personal comm., T. Abdoun, 2009). Shear forces likely develop along the tactile pressure sensors during spin-up as a result of small sand settlements (while the caisson is stationary) that occur as the model spins-up and the overburden pressures increase.

In addition to these tests, Illinois and RPI personnel conducted a simple, direct shear test to preliminarily evaluate the effect of shear stress on measured normal stress. In this test, we placed a stiff aluminum plate on the carpeted concrete floor, followed by a relatively thick, stiff rubber mat, the tactile pressure sensor, another rubber mat, and finally a thick, rigid, aluminum block roughly the size of the tactile pressure sensor. The materials and test set-up are shown in Fig. 7 and Fig. 8, respectively. The tactile pressure sensor, software, and data acquisition system were activated, and a researcher stood atop the thick aluminum block to apply normal force to the tactile pressure sensor. A shear force (in the elastic range) was then applied to the thick aluminum block (see Fig. 9).

Conditioning, or repeated load cycling, is required for proper calibration of the tactile pressure sensors. The load cycling is intended to "seat" and exercise the sensor prior to measurements. During our simple direct shear tests, normal force was measured as the researcher stood on the aluminum block. The researcher then gently bounced on the block to simulate the conditioning step, and normal force was measured again. As part of this conditioning procedure, another artifact of the tactile pressure pads was addressed: hysteresis. According to Paikowsky and Hajduk (1997), loading rate, post-loading response (creep), and hysteresis affect the pressure sensor measurements. Hysteresis is the inability of the tactile pressure pad to return to its original value after being loaded and unloaded. Although RPI is still studying this issue, the conditioning step appears to greatly reduce sensor hysteresis.

Fig. 7 Two rubber mats, thin aluminum plate, thick aluminum block, and a tactile pressure sensor used in direct shear tests.

Fig. 8 Direct shear test set-up.

Fig. 9 Conduct of direct shear test.

This test was performed on an unmodified tactile pressure sensor, a laminated sensor, a sensor with a single sheet of Teflon above the sensor, and a sensor with Teflon sheets on both sides. In all cases, the post-conditioning normal force was greater than the pre-conditioned value. Of equal interest, the normal force measured under an applied shear stress was 13% smaller in an unmodified tactile pressure sensor (compared to an unmodified sensor with no shear stress), but only 3% smaller when Teflon sheets were installed on both sides of the sensor.

As an initial theory, the reduction in normal force under an applied shear force can be explained as follows. The applied shear stresses cause the sensor's conductive material (which registers the pressure against the sensor) to become "racked." When this occurs, the area of the conductive strip becomes slightly larger, allowing more current to pass. Greater measured current corresponds to an erroneous reduction in normal force across the tactile pressure sensor.

Another test was designed to observe the effects of shear force and measured normal force and to devise a method to mitigate these effects in the centrifuge. The test used a rigid, split section box with four tactile pressure sensors of varying configuration installed on the sides (see Fig. 10 and Fig. 11). The sensors included: (1) a laminated sensor; (2) a laminated sensor with Teflon sheets front and back with vacuum grease applied between the Teflon sheets and the sensor; (3) a sensor with a single Teflon sheet on the front; and (4) a sensor with two Teflon sheets front and back, without grease between the Teflon sheets and the sensor. After the sensors were adhered to the rigid box, dry dense sand was placed in one half of the box, while saturated dense sand was placed in the other half (see Fig. 12). The box was spun-up on the centrifuge and pressures were measured. This was repeated several times after loosening the sand following spin-down.

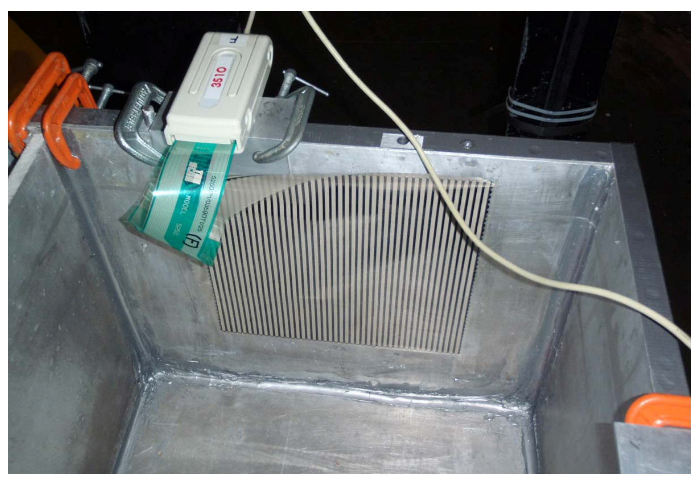

Fig. 10 Laminated tactile pressure sensor installed in rigid, split box.

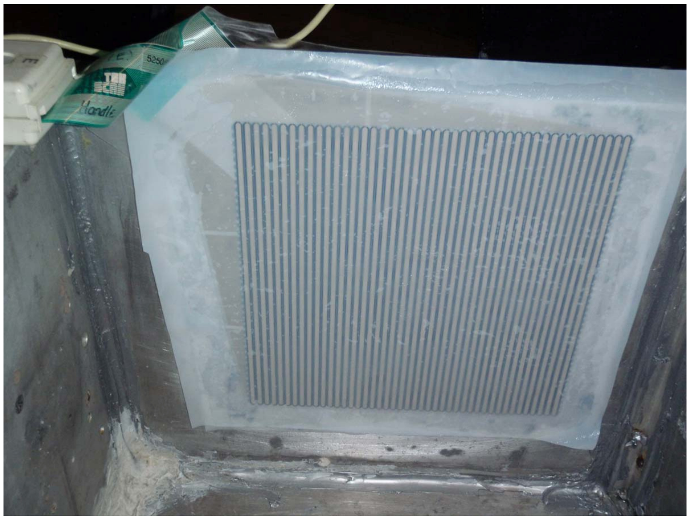

Fig. 11 Laminated tactile pressure sensor with Teflon sheeting installed front and back, with vacuum grease in-between.

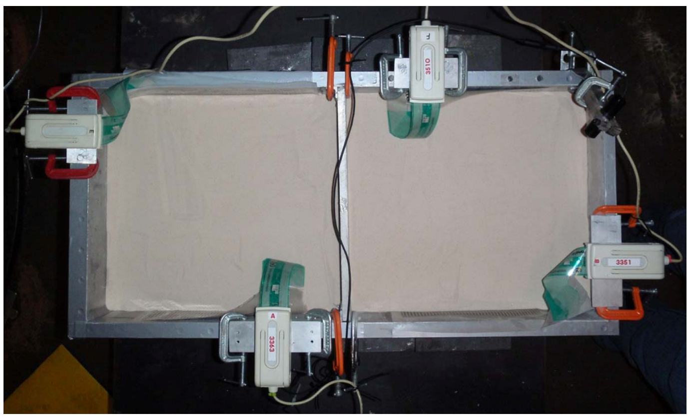

Fig. 12 Top view of split level box showing four tactile pressure sensors, each with a slightly different configuration.

Interestingly, the loose and dense sands yielded similar (reduced) values of lateral earth pressure, regardless of tactile pressure sensor configuration. We anticipate that during spin-up, consolidation of the sand produced shear forces on the tactile pressure sensor face and artificially reduced the measured lateral pressures. And although the dense sand settled less, it may have mobilized a larger shear force (as a result of its higher density) and larger friction angle.

To further investigate the effect of shear on measured normal force, the above test was repeated with the box filled with water only. This test allowed us to evaluate the measurements at low pressures and evaluate the measurement linearity (i.e., compared to the linear increase in hydrostatic pressure).

The hydrostatic centrifuge test revealed that, once again, the pressures measured by the tactile pressure sensors were less than the hydrostatic pressures. The team investigated several potential explanations including problems with the calibration technique and the long delay (typically a few days) after initial conditioning of the sensor in the calibration chamber until centrifuge testing was performed. However, we did not reach a conclusion on this issue prior to needing to perform Experiment I-A2. As a result, the project team discussed the possibility of developing an adjustment factor for the measured pressures in order to maintain our schedule.

<u>Experiment I-A2 Tactile Pressure Sensor Configuration.</u> As mentioned previously, for Experiment I-A2 the project team used a laminated Model 5250 sensor that was wrapped around and adhered to the rigid aluminum caisson as illustrated in Fig. 13 and Fig. 14. The instrumented caisson was then installed in the laminar box (see Fig. 15). Rubber mats were placed above and below the instrument handle (data collection port to the computer) and adjustable metal straps secured the handle and mats to the caisson.

In Experiment I-A2, several minor pre-shaking instrument and computer system difficulties required that the centrifuge be spun up and down several times. These activities may have had an unintended, yet beneficial consequence. As discussed later, it appears that the tactile pressures, for the first time, measured values that were reasonably consistent with the theoretical at-rest earth pressures. Spinning up and down several times appears to have conditioned the tactile pressure sensor *in situ*, making it possible for the sensor to accurately measure lateral pressures. Similar to the 1g direct shear test, the repeated spinning up and down in the centrifuge appears to have greatly reduced sensor hysteresis. This hypothesis is currently being investigated by RPI personnel in additional centrifuge tests.

EXPERIMENT I-A2 RESULTS

Experiment I-A2 was performed in the centrifuge as described earlier. The goal of this test was to measure pressures against the rigid caisson as a result of lateral spreading. While in flight, we applied a shaking motion to trigger cyclic mobility and cause downslope movement of the sand. For the purposes of this discussion, it is important to note that strains between 15% and 27% were measured within the loose sand stratum as a result of lateral spreading during the shaking event. These strains and displacements are sufficient to develop maximum pressures on the caisson (NAVFAC, 1986). The purpose of the tactile pressure sensor is to measure those pressures. The remainder of the discussion will concentrate on the results of the tactile pressure sensor, and the variations observed along the pressure pad.

<u>Tactile Pressure Sensor Measurements.</u> The tactile pressure sensor appeared to measure reasonable pressure variations with time, even considering that the frequency of the shaking, in model scale, was 50Hz. Fig. 16 shows examples of earth pressure time histories obtained at different elevations on the front face of the caisson, along with the input time history. This figure illustrates that the tactile pressure sensor recorded the same number of cycles as the input motion.

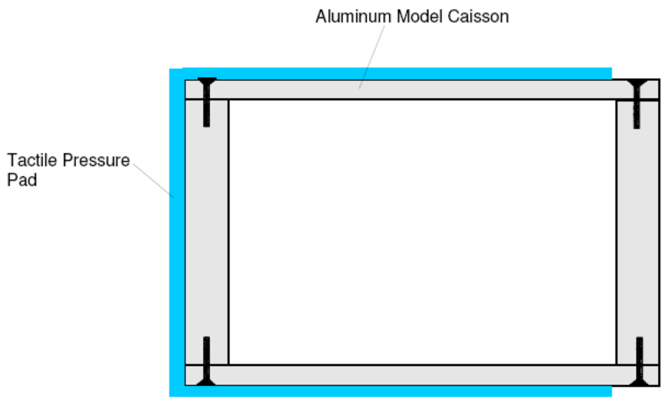

Fig. 13 Plan view of rubber membrane used as a waterproof barrier and tactile pressure sensor configuration employed in Experiment I-A2.

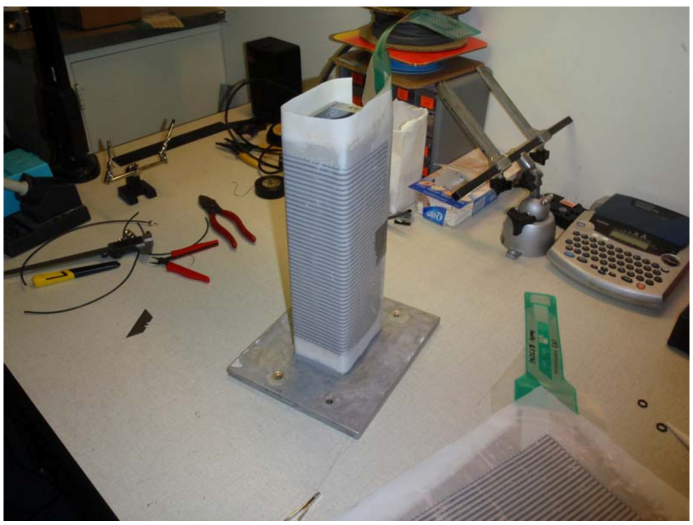

Fig. 14 Tactile pressure sensor installed on the caisson for Experiment I-A2.

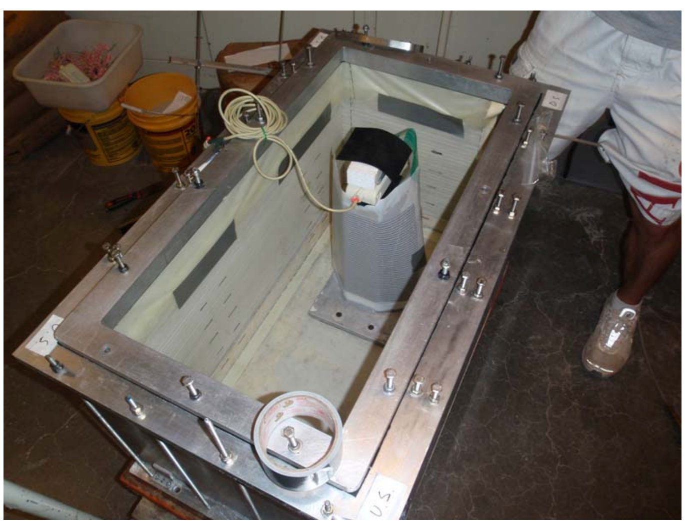

Fig. 15 Instrumented caisson installed in the laminar box for Experiment I-A2. Instrument handle is placed atop the caisson.

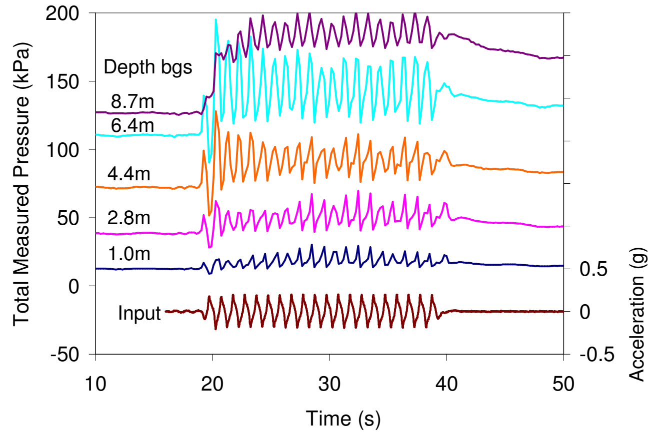

Fig. 16 Earth pressure time histories at various depths along front face of caisson.

<u>Earth Pressure Time Histories.</u> Earth pressures measured by the tactile pressure sensor were evaluated within discrete areas or clusters, where each cluster is comprised of four sensels Fig. 17 shows a screenshot of the entire tactile pressure pad (including left side, front face, and right side), with example rows including the clusters mentioned. The clusters were assigned identification numbers 1 through 22. For the configuration shown in Fig. 17, there are 16 cluster rows from the ground surface to the bottom of the tactile pressure sensor. The entire earth pressure time history for each of these clusters was extracted using the proprietary Tekscan software. Notice in this figure the color gradient from top (ground surface) to the bottom of the sensor pad (approximately 9 m below grade). The intense pressures measured near the left corner of the front face are apparently the result of a stress concentration as a result of installation of the pad on the double-sided tape on the caisson.

Fig. 18 shows the average pressures registered across the entire face of the tactile pressure pad before shaking, and Fig. 19 shows the average pressures registered across the pressure pad during shaking. Note that both figures include the high stress location at show by Cluster 9 in Fig. 17.

It should be noted that the high stresses shown at the corner were subsequently excluded from further analyses because these pressures do not represent the at-rest pressure or pressure developed during shaking. Fig. 20 shows the average pressures registered across the entire face of the tactile pressure pad before shaking with Cluster 9 eliminated. Similarly, Fig. 21 shows the average pressures registered across the pressure pad during shaking with Cluster 9 eliminated. (Note that the pressure axis scale has changed.)

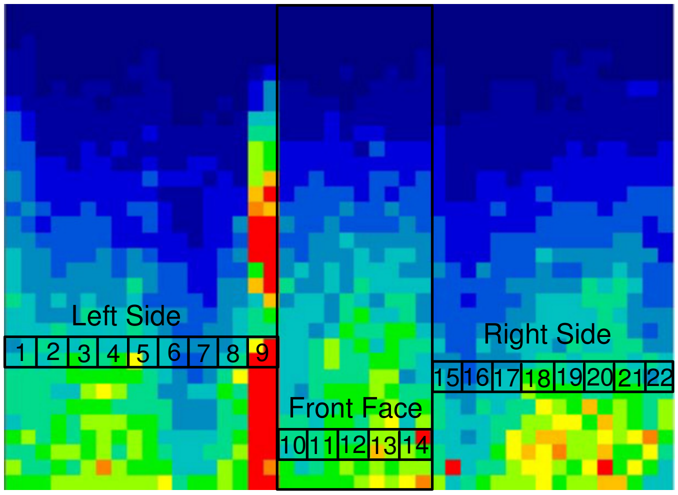

Fig. 17 Screenshot of tactile pressure sensor showing example clusters from which pressure were examined in discrete areas.

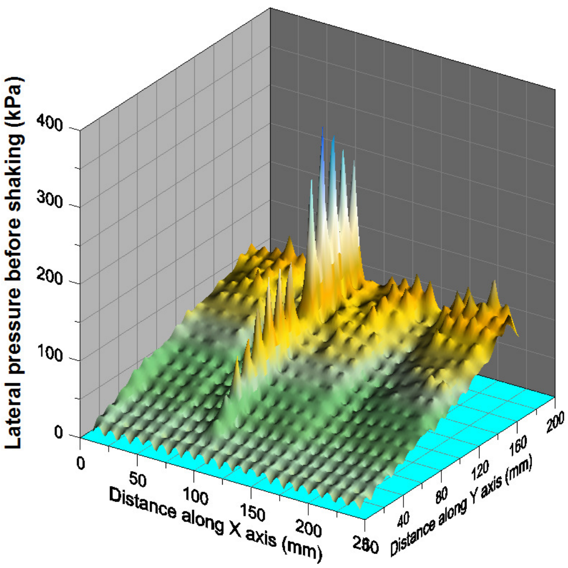

Fig. 18 *Average pressures on tactile pressure pad before shaking (including high corner stresses).*

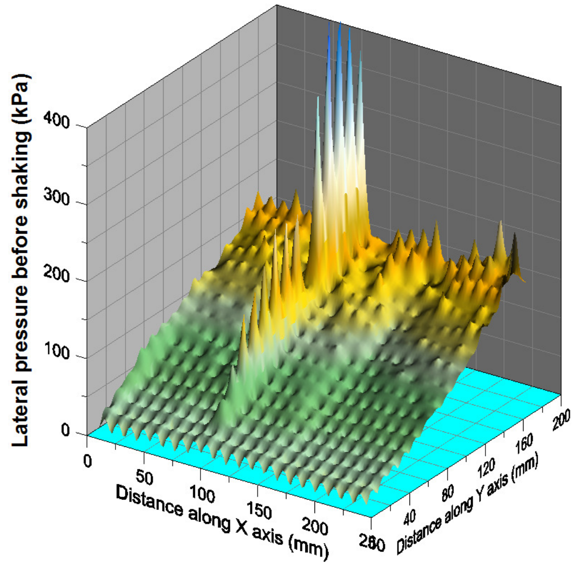

Fig. 19 *Average pressures on tactile pressure pad during shaking (including high corner stresses).*

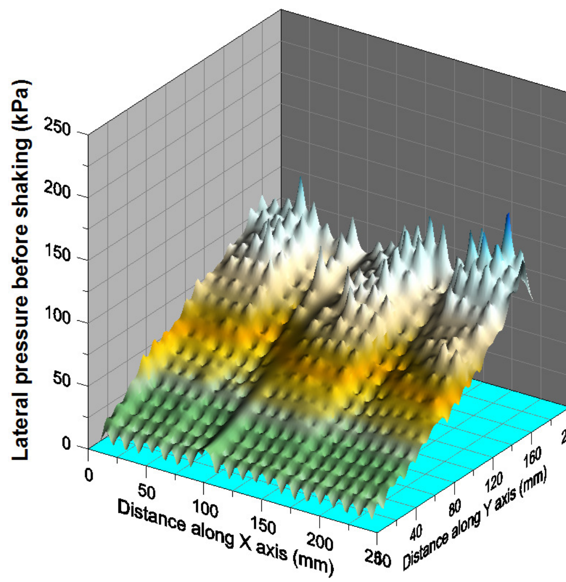

Fig. 20 Average pressures on tactile pressure pad before shaking (high corner stresses excluded).

Pressure Measurement Interpretation. Three clusters on the front face were selected for detailed interpretation: Clusters 10-14, Clusters 12-14, and Cluster 14 alone (see Fig. 17). Clusters 10-14 represent the overall average earth pressure across the face of the caisson. Clusters 12-14 were selected to provide an estimate of variability with respect to Cluster 10-14, and Cluster 14, alone was selected because this column appeared to exhibit the largest earth pressures on the caisson face.

Fig. 22, Fig. 23, and Fig. 24 present overviews of lateral earth pressures measured on the caisson face using three different configurations of cluster as described above. The plots include average pressures developed prior to shaking, during shaking, and after shaking,. For comparison, the approximate at-rest, Rankine active, Rankine drained passive, and Rankine undrained passive earth pressures are included in these figures as well.

The earth pressure distributions shown in Fig. 22 and Fig. 23 exhibit relatively smooth increases in earth pressure with depth, whereas Fig. 24 exhibits a relatively variable pressure distribution before shaking, during shaking, and after shaking. This illustrates the idea that use of a single cluster arrangement may result in misleading earth pressures.

As illustrated in Fig. 22 and Fig. 23, the measured lateral pressures prior to shaking agree well with theoretical at-rest earth pressures. As mentioned previously, we anticipate that the conditioning of the tactile pressure sensor *in situ* during repeated spin ups and spin downs prior to shaking may be responsible for the satisfactory lateral pressures measured. In addition, the average earth pressure measured during shaking agrees closely with the Rankine undrained passive earth pressure when the undrained passive pressure is computed using a liquefied strength ratio, $s_u(liq)/\sigma'_{vo}$, of 0.10 following the Olson and Stark (2002) correlation.

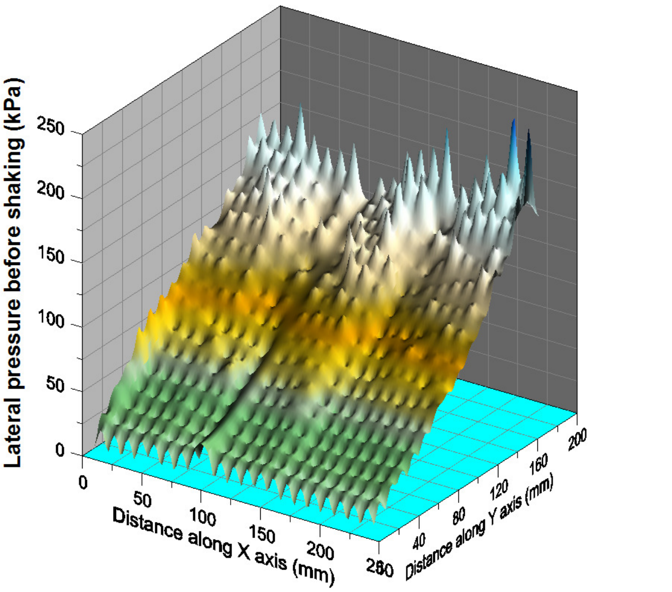

Fig. 21 Average pressures on tactile pressure pad during shaking (high corner stresses excluded).

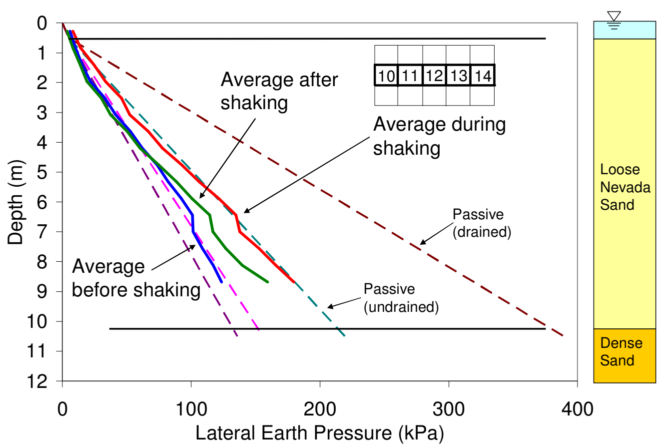

Fig. 22 Pressure distribution with depth using and average of Clusters 10 through 14.

SUMMARY AND CONCLUSIONS

Centrifuge tests were conducted to measures lateral earth pressure during liquefaction-induced lateral spreading against a large, rigid foundation element. For this purpose, tactile pressure sensors were employed for the first time in a saturated, dynamic centrifuge environment. Several lessons about the use of the tactile pressure sensors in this environment were learned, and the early challenges encountered seem to be resolved. However, Interpretation of the pressures measured across the tactile pressure sensor and interpretation of the variation of measurements and response during shaking is ongoing.

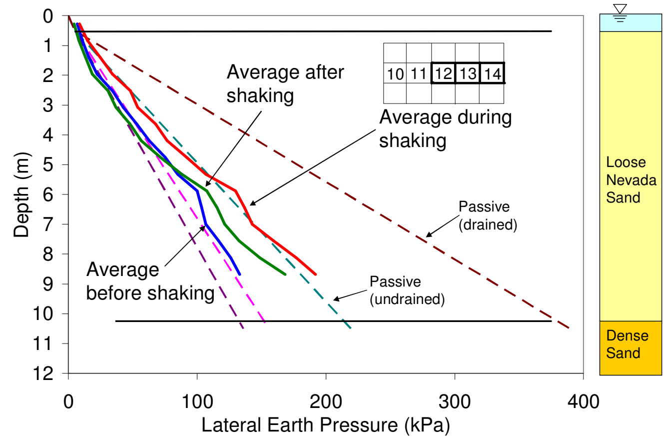

Fig. 23 Pressure distribution with depth using and average of Clusters 12 through 14.

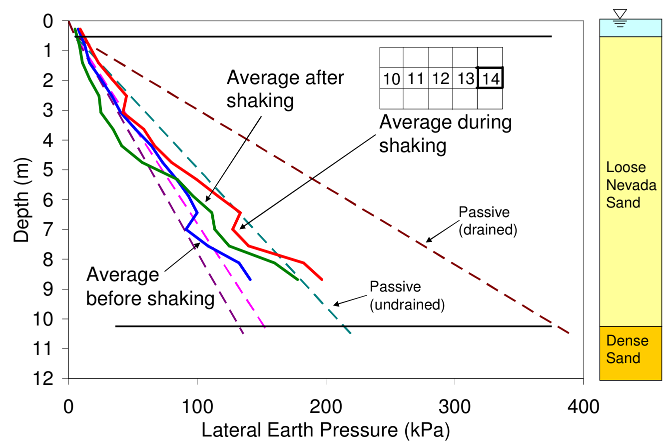

Fig. 24 Pressure distribution with depth using Cluster 14 only.

Two ingredients appear to be essential to the good performance of tactile pressure sensors: (1) use of a low friction material on the tactile pressure pad (Teflon); and (2) use of a conditioning procedure performed *insitu* within the laminar box prior to shaking.

The use of the laminated tactile pressure sensors combined with vacuum grease on each side, and sandwiched by a Teflon sheet on either side of the caisson likely also contributed to the apparent success with the tactile pressure sensor. The tactile pressure sensor (sandwiched between the Teflon sheets) was adhered directly to the caisson face using thin double sided tape. Because a rather smooth pressure gradient was observed on the tactile pressure sensor, we anticipate that this configuration yielded good compliance between this pressure sensor and the rigid caisson.

Conditioning the tactile pressure sensors *insitu* appears to mitigate the effect of sensor hysteresis and promotes more accurate lateral pressure measurements under geostatic conditions and perhaps during dynamic conditions.

ACKNOWLEDGMENTS

This project is being funded by NEES under Contract No. 1-490538-191100 (2008), NSF CMMI 07-2369. This support is gratefully acknowledged. The support and cooperation of the centrifuge facility staff at RPI is also very much appreciated during this testing.

REFERENCES

Arumoli, K., Muraleetharan, K.K., Hossain, M.M., Fruth, L.S., (1992). "Verification of Liquefaction Analysis by Centrifuge Studies Laboratory Program Soil Data," Report; The Earth Technology Corporation.

Kutter, B.L., (1995). "Recent Advances in Centrifuge Modeling of Seismic Shaking," State-of-the-Art Paper, Preceedings, Third International Conference on Recent Advances in Geotechnical Earthquake Engineering and Soil Dynamics, St. Louis, MO, Vol. 2, pp. 927-942.

NAVFAC, Design Manual 7.02, (1986), *Foundations and Earth Structures*, Naval Facilities Engineering Command, Alexandria, Virginia, 279pp.

Olson, S.M. and Stark, T.D., (2002). "Liquefied Strength Ratio from Liquefaction Flow Failure Case Histories," Canadian Geotechnical Journal, Vol. 40, No. 6, pp. 1164-1184.

Paikowsky, S.G. and Hajduk, E.L., (1997). "Calibration and Use of Grid-Based Tactile Pressure Sensors in Granular Material," Geotechnical Testing Journal, Vol. 20, No. 2, pp. 218-241.